THE JOURNAL OF PHYSICAL CHEMISTRY B

 VOLUME 108, NUMBER 11, MARCH 18, 2004

LETTERS

Aligned TiO_2 Nanorods and Nanowalls

Jih-Jen Wu* and Chi-Chung Yu

Department of Chemical Engineering, National Cheng Kung University, Tainan, Taiwan

Received: July 28, 2003; In Final Form: December 9, 2003

Well-aligned rutlie and anatase TiO_2 nanorods as well as anatase TiO_2 nanowalls have been synthesized using a template- and catalyst-free metalorganic chemical vapor deposition (MOCVD) method. Structural analyses indicate that single-crystalline rutile and anatase TiO_2 nanorods were formed at 630 °C and 560 °C, respectively, while anatase TiO_2 nanowalls composed of well-aligned nanorods were formed at 535 °C. Optical characterizations of these TiO_2 nanostructures show that the band gap energies for indirect transistion of the rutile TiO_2 nanorods and anatase TiO_2 nanorods as well as nanowalls are at 3.0 and 3.2 eV, respectively.

Titanium dioxide is a versatile material and has been investigated considerably due to its unique optoelectronic and photochemical properties, such as high refractive index, high dielectric constant, excellent optical transmittance in the visible and near-IR region as well as high performance photocatalysis for water splitting and for degradation of organics.[1] TiO_2 has also been demonstrated as a promising electron-transport material of a dye-sensitized oxide semiconductor solar cell.[2] Nanocrystalline or porous films are used in the photoelectrochemical cells due to their high surface areas. Moreover, ferromagnetic Co-doped TiO_2 films have been reported to possess a Curie temperature higher than 400 K.[3] Crystalline TiO_2 exists in three structures: rutile (tetragonal), anatase (tetragonal), and brookite (orthorhombic). Among them, rutile is the most stable phase while anatase possesses superior optoelectronic and photocatalytic properties.[1] Recently, the use of one-dimensional (1-D) nanostructures instead of nanocrystalline films in photoelectrochemical cells has been considered.[4,5] 1-D CdSe nanorods have been demonstrated to be preferable to the nanocrystalline films in solar energy conversion because of their single-crystal structures providing a directed path for electron transport.[4] In addition, a more than 2-fold increase in maximum photoconversion efficiency for water splitting has been observed by replacing TiO_2 nanocrystalline films with TiO_2 nanowires.[5] Growth of 1-D TiO_2 nanostructures, including nanowires and nanotubes, has been demonstrated using sol−gel, electrodeposition, and hydrothermal methods with or without anodic aluminum oxide (AAO).[6] TiO_2 nanorods have also been grown on a WC−Co substrate by metalorganic chemical vapor deposition (MOCVD) using titanium-tetraisopropoxide (TTIP) as the precursor.[7] An energy dispersive spectrum of the nanorods showed the presence of Co with Ti and O. The presence of Co was suggested to catalyze the formation of the TiO_2 nanorods.[7] Here we present a simple MOCVD approach to the template- and catalyst-free growth of aligned TiO_2 nanostructures, i.e., rutile and anatase nanorods as well as anatase nanowalls, on fused silica and Si(100) substrates. Both rutile and anatase TiO_2 nanorods possess the single crystalline structures. The aligned TiO_2 nanostructures grown on the substrates directly may possess potentials for photoelectrochemical and optoelectronic applications.

TiO_2 nanostructures were grown in a two-temperature-zone furnace. Titanium metalorganic precursor, titanium acetylacetonate ($Ti(C_{10}H_{14}O_5)$, Merck, >97%), placed on a Pyrex glass container was loaded into the low-temperature zone of the furnace which was controlled to be at 200−230 °C to vaporize the solid reactant. The vapor was carried by a 1000-sccm N_2/O_2 flow into the high-temperature zone of the furnace in

* Corresponding author. E-mail: wujj@mail.ncku.edu.tw.

10.1021/jp0361935 CCC: $27.50
Published on Web 02/19/2004

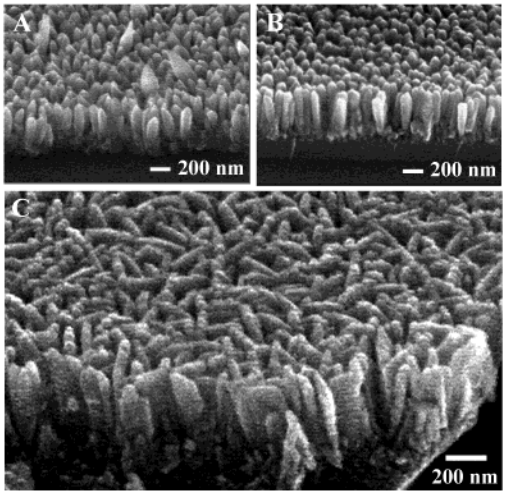

Figure 1. (A−C) 45°-tilted SEM images of TiO_2 nanostructures grown at 630 °C, 560 °C, and 535 °C, respectively.

which substrates were located. TiO_2 nanostructures were grown directly on bare fused silica or silicon substrates at a temperature of 500−700 °C. Figures 1(A)−(C) show TiO_2 nanostructures grown on fused silica substrates using the template- and catalyst-free MOCVD method. Well-aligned nanorods, as shown in Figures 1(A) and (B), are formed at 630 °C and 560 °C under a pressure of 5 Torr. Aligned two-dimensional nanostructures, so-called nanowalls, are grown at lower temperature and pressure of 535 °C and 3.6 Torr, respectively, as shown in Figure 1(C). It reveals that a piece of nanowall consists of several well-aligned nanorods grown in a line, resulting in the morphology of the 2-D nanostructures. Similar nanostructures were also formed on Si(100) substrates at the three temperatures.

The crystal structures of the aligned TiO_2 nanostructures were characterized by X-ray diffraction (XRD). Figure 2(A) shows XRD patterns of the aligned nanostructures grown on fused silica substrates at the three temperatures. These spectra are compared with the rutile and anatase TiO_2 powder diffraction profiles, JCPDS No. 77-041 and No. 83-2243. Pattern I in Figure 2 indicates that the TiO_2 nanorods grown at 630 °C possess the rutile structure with a preferential orientation of (110). The XRD pattern shown in pattern II illustrates the formation of the anatase phase TiO_2 nanorods at 560 °C and (220) preferential orientation of the antanse TiO_2 nanorods. Pattern III shows the antanse structure of the TiO_2 nanowalls grown at 535 °C with a preferential orientation of (200). Further structural characterizations of the TiO_2 nanostructures were performed using transmission electron microscopy (TEM). Figure 2(B) shows a TEM image of a TiO_2 nanorod grown at 560 °C as well as the corresponding electron diffraction patterns (inset). No additional metal particle appearing on the top of the nanorod, indicating a non-VLS approach to the growth of the aligned TiO_2 nanorods, was achieved. The diffraction pattern confirms the XRD analysis that the anatase TiO_2 nanorods were formed at 560 °C. It also reveals that the anatase TiO_2 nanorod possesses the single-crystalline structure. Figure 2(C) shows a high-resolution TEM image of an anatase TiO_2 nanorod. The lattice spacing of 0.26 nm in the longitudinal direction corresponds to the *d* spacing of (110) crystal planes, confirming the XRD analysis that the anatase TiO_2 nanorods are preferentially oriented in the [110] direction. TEM analyses also show single-crystalline rutile TiO_2 nanorods formed at 630 °C. Figure 2(D) shows a TEM image of a TiO_2 nanowall grown at 535 °C as well as the corresponding electron diffraction patterns (inset). It reveals that a nanowall

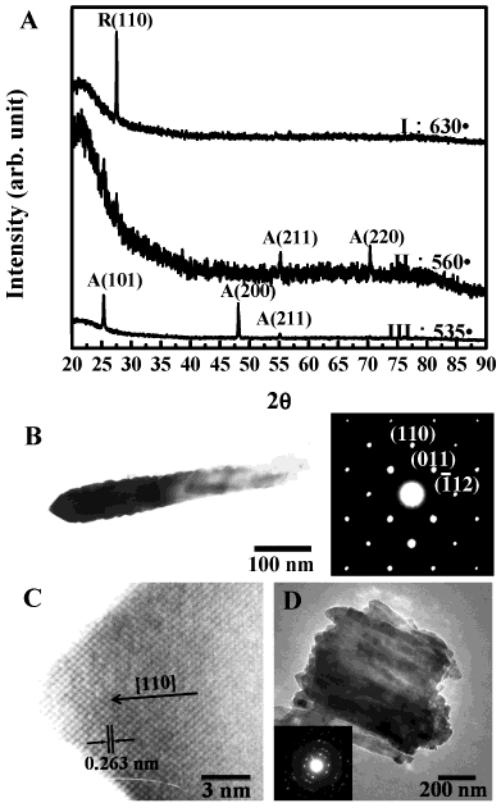

Figure 2. (A) XRD spectra of the TiO_2 nanostructures. (B) TEM image of an anatase TiO_2 nanorod and the corresponding electron diffraction pattern. (C) High-resolution image of the nanorod in (B). (D) TEM image of a TiO_2 nanowall and the corresponding electron diffraction pattern (inset).

is composed of several nanorods, consistent with the SEM observation. The *d* spacings observed from the diffraction pattern confirm the anatase TiO_2 structure of the nanowall.

Optical properties of the aligned TiO_2 nanostructures on fused silica substrates are investigated by UV−visible spectrophotometer. The UV−visible absorption measurements, as shown in Figure 3, indicate that the TiO_2 nanorods and nanowalls are transparent in the visible range. Assuming that the fundamental absorption of the TiO_2 crystal possesses an indirect transition,[1] the band edge energies of the three TiO_2 nanostructures are evaluated by plotting $(\alpha E)^{1/2}$ (where α and E represent the absorption coefficient and photoenergy, respectively) against *E*.[8] As shown in the insets of Figures 3(A)−(C), the intercepts defining the energy gaps for the rutile TiO_2 nanorods and the anatase TiO_2 nanorods are 3.0 and 3.2 eV, respectively. The anatase TiO_2 nanowalls also possesses an indirect band gap of 3.2 eV estimated by the same method.

A possible mechanism for the formation of the well-aligned TiO_2 nanorods by the template- and catalyst-free MOCVD approach is proposed to correspond to the relative growth rate of various crystal faces bounding the tetragonal TiO_2 nanocrystal. For a crystal with an anisotropic crystallographic structure, the direction of the crystal face with the corner of the coordination polyhedron occurring at the interface possesses the fast growth rate, and the directions of the crystal face with the edge and with the face of the coordination polyhedron occurring at the interface have the second fastest and the slowest growth rates, respectively.[8] Moreover, the growth habit of the crystal is mainly determined by the internal structures of a given crystal and is also affected by growth conditions.[9] According to the structural analyses of the anatase TiO_2 nanorod, we propose

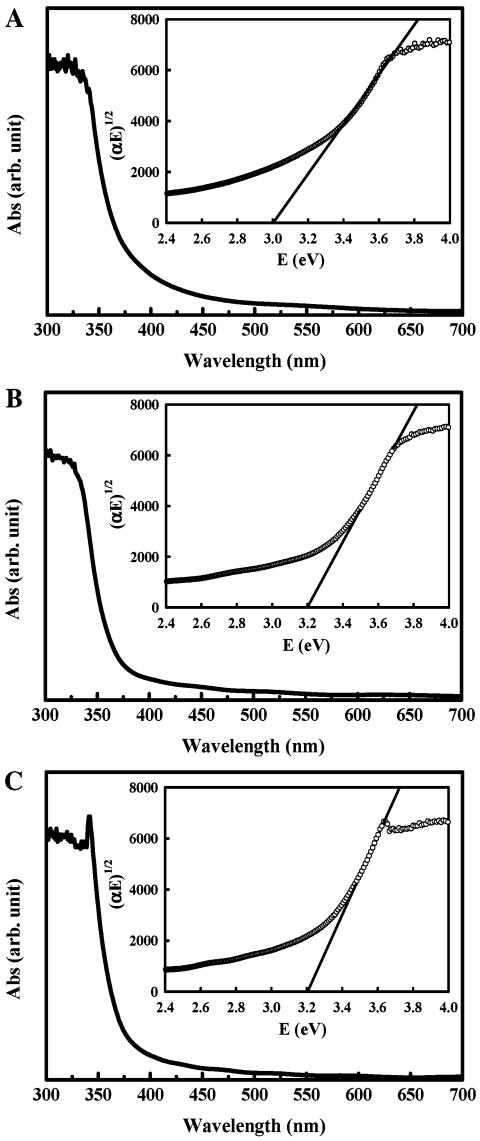

Figure 3. Room-temperature absorption spectra of the (A) rutile TiO_2 nanorods, (B) anatase TiO_2 nanorods, and (C) anatase TiO_2 nanowalls. The insets show the dependence of the absorption coefficient as a function of $h\nu$ for the TiO_2 nanostructures.

that the relationship of the growth rates of the TiO_2 crystal faces is $R_{(110)} > R_{(011)} > R_{(\bar{1}12)}$, resulting in the aligned anatase TiO_2 nanorods with a preferential orientation of (110) formed on silicon or fused silica substrates, as schematized in Figures 4. On the other hand, the distinction of the preferential orientation of the anatase TiO_2 nanowalls from that of the anatase TiO_2 nanorods is ascribed to the variation of the growth conditions. Since there are nanocrystals appearing in front of the nanowalls

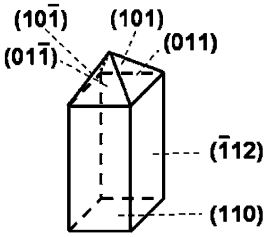

Figure 4. The growth habit schematic of the anatase TiO_2 nanorods in this study.

in the cross-sectional region of Figure 1(C), it is thus suggested that the nanowalls were separated by nanocrystals in consequence the network construction of the aligned nanowalls on the substrates.

In summary, we have demonstrated the formation of the aligned rutile and anatase TiO_2 nanorods as well as anatase TiO_2 nanowalls by a template- and catalyst-free MOCVD method. Structural analyses indicate that single-crystalline rutile and anatase TiO_2 nanorods were formed at 630 °C and 560 °C, respectively, while anatase TiO_2 nanowalls composed of well-aligned nanorods were formed at 535 °C. Optical characterizations of the TiO_2 nanostructures show that the absorption edges of the rutile TiO_2 nanorods and anatase TiO_2 nanorods as well as nanowalls are at 3.0 and 3.2 eV, respectively. Formation of the well-aligned TiO_2 nanorods is proposed to correspond to the relative growth rate of various crystal faces bounding the tetragonal TiO_2 nanocrystal.

Acknowledgment. The authors thank Prof. Y. Chen for help with absorption analyses. Financial support from the National Science Council in Taiwan under Contract No. NSC 91-2214-E-006-012 is gratefully acknowledged.

References and Notes

(1) Diebold, U. *Surf. Sci. Rep.* **2003**, *48*, 53.
(2) Gratzel, M. *Nature* **2001**, *414*, 338.
(3) Matsumoto, Y.; Murakami, M.; Shono, T.; Hasegawa, T.; Fukumura, T.; Kawasaki, M.; Ahmet, P.; Chikyow, T.; Koshihara, S.; Koinuma, H. *Science* **2001**, *291*, 854.
(4) Huynh, W. U.; Dittmer, J. J.; Alivisatos, A. P. *Science* **2002**, *295*, 2425.
(5) Khan, S. U. M.; Sultana, T. *Sol. Energy Mater. Sol. Cells* **2003**, *76*, 211.
(6) Lakshmi, B. B.; Dorhout, P. K.; Martin, C. R. *Chem. Mater.* **1997**, *9*, 857. (b) Kasuga, T.; Hiramatsu, M.; Hoson, A.; Sekino, T.; Niihara, K. *Langmuir* **1998**, *14*, 3160. (c) Zhang, X. Y.; Zhang, L. D.; Chen, W.; Meng, G. W.; Zheng, M. J.; Zhao, L. X. *Chem. Mater.* **2001**, *13*, 2511. (d) Kasuga, T.; Hiramatsu, M.; Hoson, A.; Sekino, T.; Niihara, K. *Adv. Mater.* **1999**, *11*, 1307.
(7) Pradhan, S. K.; Reucroft, P. J.; Yang, F.; Dozier, A. *J. Crystal Growth* **2003**, *256*, 83.
(8) Pankove, J. I. *Optical Processes in Semiconductor*; Prentice Hall: New York, 1971.
(9) Laudise, R. A.; Ballman, A. A. *J. Phys. Chem.* **1960**, *64*, 688. (b) Li, W. J.; Shi, E. W.; Zhong, W. Z.; Yin, Z. W. *J. Cryst. Growth* **1999**, *203*, 186.